nature publishing group

Neonatal monocytes express antiapoptotic pattern of Bcl-2 proteins and show diminished apoptosis upon infection with *Escherichia coli*

Anja Leiber[1], Benjamin Graf[1], Bärbel Spring[1], Justine Rudner[2], Natascha Köstlin[1], Thorsten W. Orlikowsky[3], Christian F. Poets[1] and Christian Gille[1]

BACKGROUND: Neonates show sustained inflammation after a bacterial infection, which is associated with inflammatory diseases like bronchopulmonary dysplasia or periventricular leucomalacia. Physiologically, inflammation is terminated early after the removal of the invading pathogens by phagocytosis-induced cell death (PICD) of immune effector cells. Earlier results showed reduced PICD in neonatal monocytes. The underlying molecular mechanisms are unknown. We hypothesize that the reduced PICD in neonatal monocytes is regulated through the proteins of the B-cell lymphoma 2 (Bcl-2) protein family.

METHODS: mRNA and protein expression of Bcl-2 family proteins in cord blood and adult peripheral blood monocytes infected with *Escherichia coli* were analyzed by quantitative real-time PCR and flow cytometry and cytochrome c release by fluorescence microscopy.

RESULTS: mRNA expression of antiapopototic Bcl-xL was upregulated in cord blood monocytes (CBMO), whereas pro-apoptotic Bim tended to be higher in peripheral blood monocytes (PBMO). Upon infection, Bax was more strongly expressed in PBMO compared with CBMO. The pro/antiapoptotic balance was skewed toward survival in CBMO and apoptosis in PBMO. Cytochome c release into the cytosol was enhanced in PBMO compared with CBMO.

CONCLUSION: Bcl-2 proteins are involved in reduced PICD in neonatal monocytes. These findings are another step toward the understanding of sustained inflammation in neonates.

Neonatal sepsis is a major health problem and an important cause of morbidity and mortality in term and preterm neonates (1). While the acute infection can be terminated in many cases, the accompanying inflammation is hardly controllable and may outlast the acute disease (2). The "sustained inflammation" (3) may predispose to inflammatory diseases like periventricular leukomalacia or bronchopulmonary dysplasia, often leading to lifelong sequelae (4,5). While clinical characteristics of these diseases are well known, their pathophysiology leading to organ damage is still poorly understood (3).

Monocytes and macrophages are key effector cells during bacterial infection. They phagocytose bacteria to eliminate pathogens and may orchestrate the following immune reaction by cytokine release and antigen presentation to the adaptive immune system (6). Under physiological conditions, monocyte activity is terminated by apoptosis (7), mainly induced by phagocytosis and, therefore, called phagocytosis-induced cell death (PICD) (8,9). PICD has been shown to occur after infection with a variety of different pathogens, including *Escherichia coli* and group-B-*Streptococci*, two of the main causative agents of neonatal sepsis (9). PICD of monocytes and apoptosis of other immune cells are important for terminating inflammation (10). A former study in adult septic patients showed a poor outcome in patients with reduced monocyte apoptosis (11).

Apoptosis can be induced by at least two major pathways: the extrinsic apoptosis pathway involves death ligands binding to their receptors, leading to activation of caspase 8, and the intrinsic pathway, regulating mitochondrial membrane permeabilization and cytochrome c release through proteins of the B-cell lymphoma 2 (Bcl-2) protein family and leading to activation of caspase 9. Both pathways result in activation of caspase 3 and DNA fragmentation (10) and are involved in PICD (12,13).

The Bcl-2 protein family consists of pro (Bax, Bak, Bim, and Bid) and antiapoptotic (Bcl-2 and Bcl-xL) members. Bax and Bak can form pores in the outer mitochondrial membrane and lead to the release of cytochrome c from the mitochondrial intermembrane space (14). Bax and Bak are inhibited by the antiapoptotic proteins of the family, such as Bcl-2 and Bcl-xL (15). Bim and Bid can inactivate Bcl-2 and Bcl-xL, which leads to reduced inhibition of Bax and Bak (16), while Bax and Bak become directly activated by Bim and Bid (17).

In the previous studies, we found that cord blood monocytes (CBMO) did not differ from peripheral blood monocytes (PBMO) of healthy adults in phagocytosis

[1]Department of Neonatology, University of Tuebingen, Tuebingen, Germany; [2]Institute for Cell Biology, University of Essen, Essen, Germany; [3]Department of Neonatology, University of Aachen, Aachen, Germany. Correspondence: Christian Gille (christian.gille@med.uni-tuebingen.de)

Received 20 August 2013; accepted 13 February 2014; advance online publication 18 June 2014. doi:10.1038/pr.2014.74

(see **Supplementary Figure S1** online) and degradation of bacteria (18) but showed strongly decreased PICD after infection with *E. coli* compared with PBMO (8), with the surviving monocytes showing proinflammatory activity (8,18). The CD95L pathway of apoptosis was shown to be crucial for monocyte apoptosis after bacterial infection. However, CD95L secretion was strongly reduced in CBMO, while external CD95L could restore CBMO apoptosis (8,13).

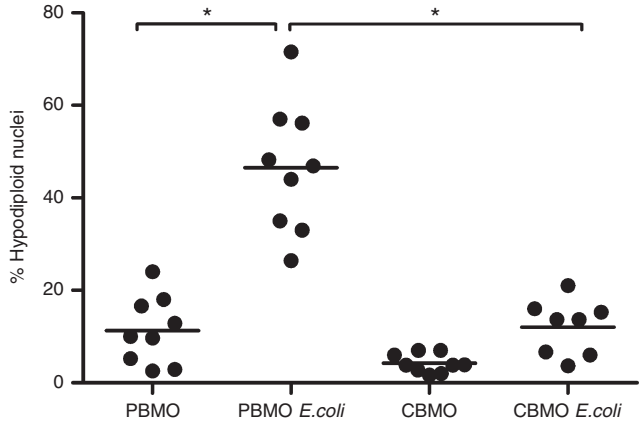

Figure 1. Apoptosis upon infection with *E. coli*-GFP was diminished in CBMO vs. PBMO. PBMO and CBMO were infected with *E. coli*-GFP for 1 h as described. Cells were incubated for 24 h, and the percentage of hypodiploid nuclei was analyzed by flow cytometry ($n = 8$) (*$P < 0.05$). CBMO, cord blood monocytes; GFP, green fluorescent protein; PBMO, peripheral blood monocytes.

In this study, we have analyzed the involvement of the intrinsic apoptosis pathway in PICD of monocytes exposed to *E. coli* and hypothesized that the regulation of this pathway through proteins of the Bcl-2 family may be different in CBMO compared with PBMO. We show that CBMO expressed higher levels of antiapoptotic proteins compared with PBMO, while the expression of proapoptotic proteins was diminished in CBMO. Cytosolic distribution of cytochrome c after infection with *E. coli* was seen in PBMO and CBMO, and in PBMO to a significantly higher extent. These results suggest an involvement of both the intrinsic and the extrinsic apoptosis pathways in reduced PICD in neonatal monocytes and may be another key mechanism to understanding sustained inflammation in neonates.

RESULTS

Expression of Antiapoptotic Bcl-xL Was Upregulated in CBMO After Infection With *E. coli*-Green Fluorescent Protein

In CBMO, apoptosis was rare after infection with *E. coli*-green fluorescent protein (GFP), confirming earlier results (8) (**Figure 1**).

To identify the role of pro and antiapoptotic proteins of the Bcl-2 protein family in this process, we studied mRNA regulation of Bcl-2 proteins known to be important in monocytes in PBMO and CBMO after infection with *E. coli*-GFP. Two hours after infection with *E. coli*-GFP Bcl-xL mRNA was upregulated 2.6-fold (±0.65) compared with uninfected control cells in CBMO ($n = 4$; $P < 0.05$; **Figure 2a**). No change in Bcl-xL

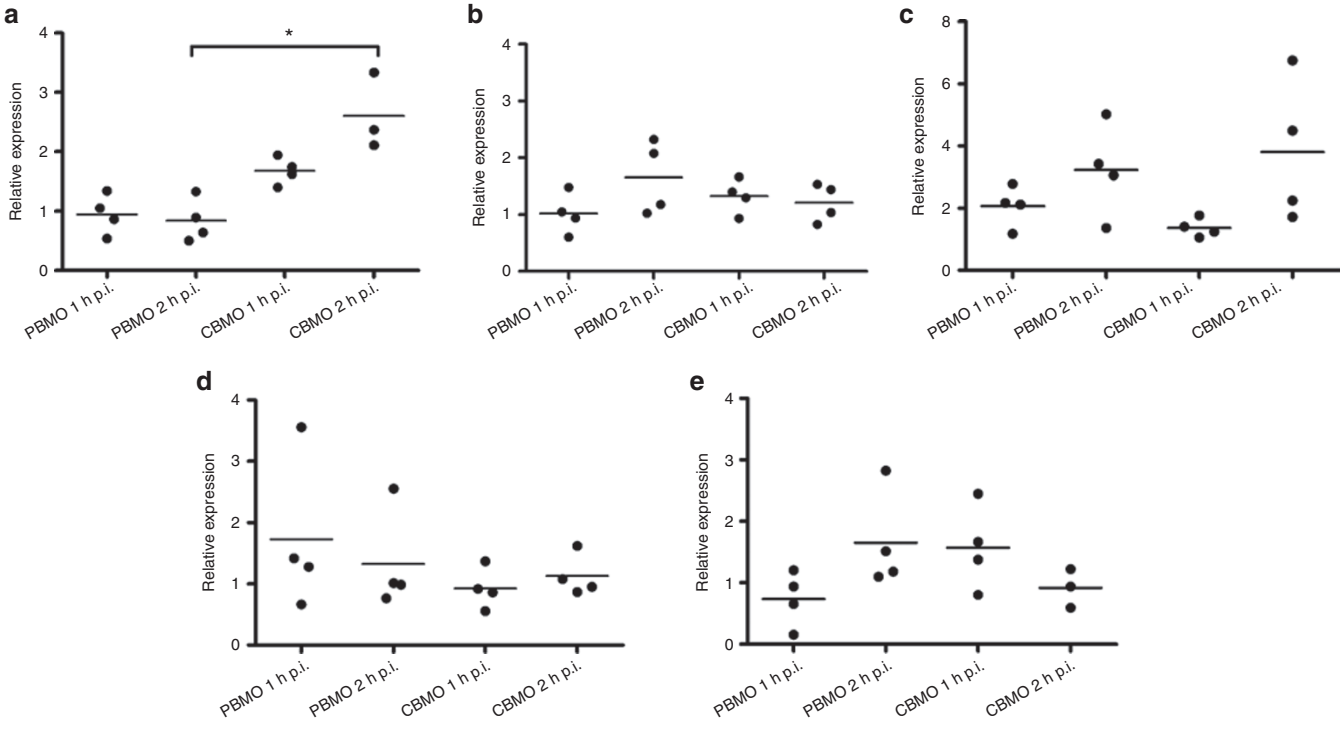

Figure 2. Bcl-xL was upregulated in CBMO, Bim was upregulated in PBMO and CBMO after infection with *E. coli*-GFP. PBMO and CBMO were infected with *E. coli*-GFP for 1 h. After 1 h and 2 h of further incubation, relative mRNA levels of (**a**) Bcl-xL, (**b**) Mcl-1, (**c**) Bim, (**d**) Bid, and (**e**) Bax were analyzed by quantitative real-time PCR ($n = 4$) (*$P < 0.05$). Bcl, B-cell lymphoma; CBMO, cord blood monocytes; GFP, green fluorescent protein; PBMO, peripheral blood monocytes.

mRNA was seen in PBMO. No significant mRNA regulation was found for mRNA of the antiapoptotic protein Mcl-1 (Figure 2b).

mRNA of the proapoptotic protein Bim tended to be upregulated in PBMO and CBMO (Figure 2c), while there was no regulation of Bid- and Bax-mRNA (Figure 2d,e).

The Pro/antiapoptotic Balance Was Skewed to the Antiapoptotic Side in CBMO After Infection With *E. coli*-GFP

To determine the pro/antiapoptotic balance of Bcl-2 proteins after infection with *E. coli*-GFP, we calculated quotients of pro and antiapoptotic proteins, which seemed to be regulated in monocytes. For CBMO, the quotient of proapoptotic Bax to antiapoptotic Bcl-xL was 0.27 (±0.11; $n = 4$), which means that the pro/antiapoptotic balance was on the antiapoptotic side (Table 1). For PBMO, the balance was on the proapoptotic side with a relative expression of Bax mRNA to Bcl-xL mRNA of 2.15 (±0.94; $n = 4$; $P < 0.05$ CBMO vs. PBMO). The proapoptotic side was even more dominant in PBMO if we used the quotient of Bim mRNA to Bcl-xL mRNA (4.21 ± 2.36; $n = 3$). For CBMO, this quotient was 1.07 (±0.67; $n = 4$; $P < 0.05$ PBMO vs. CBMO).

Infection With *E. coli*-GFP Had No Influence on Bcl-xL Protein Expression

To investigate if the regulation of mRNA would be translated to protein level, we analyzed Bcl-family-proteins in PBMO and CBMO after infection with *E. coli*-GFP by flow cytometry. Bcl-xL expression remained unchanged upon infection in both, PBMO (mean fluorescence intensity (MFI): 13.7 ± 2.9 vs. 12.5 ± 4.1 after 1 h of further incubation and 15.0 ± 10.2 after 4 h of further incubation; $n = 6$ for 1 h and $n = 5$ for 4 h; Figure 3a) and CBMO (MFI: 9.5 ± 2.8 vs. 8.3 ± 2.6 after 1 h of further incubation and 7.8 ± 5.7 after 4 h of incubation; $n = 6$ for 1 h and $n = 5$ for 4 hours; Figure 3a). Compared with uninfected cells, the percentage of Bcl-xL–positive cells seemed to be slightly diminished after infection with *E. coli*-GFP after 1 h of further incubation in CBMO (95.7 ± 2.1 vs. 89.2 ± 5.2%; $n = 6$; $P > 0.05$; Figure 3b) but not after 4 h of further incubation nor in PBMO.

In monocytes, Bcl-xL can be localized either in the cytosol or at the outer mitochondrial membrane, depending on the apoptotic status of the cell (15,19). Intracellular localization of Bcl-xL was analyzed by fluorescence microscopy. In PBMO and CBMO, Bcl-xL was colocalized with mitochondria (Figure 3c,d). After infection with *E. coli*-GFP, Bcl-xL was distributed to the whole cytosol.

Table 1. In PBMO, the pro/antiapoptotic balance drifted to the proapoptotic side after infection with *E. coli*-GFP

Ratio	PBMO	CBMO
Bax/Bcl-XL	2.15 ± 0.94	0.27 ± 0.11*
Bim/Bcl-XL	4.21 ± 2.36	1.07 ± 0.67*

Pro/antiapoptotic quotients were calculated from relative mRNA expression.
Mean ± SD is given.
Bcl, B-cell lymphoma; CBMO, cord blood monocytes; GFP, green fluorescent protein; PBMO, peripheral blood monocytes.
*$P < 0.05$ for PBMO vs. CBMO.

Bax Protein Expression Was Increased in PBMO After Infection With *E. coli*-GFP

Intracellular protein expression of Bax was analyzed by flow cytometry. After infection with *E. coli*-GFP, mean fluorescence intensity of Bax increased in PBMO (52.3 ± 7.7 vs. 14.2 ± 7.4 after 1 h of incubation; $n = 6$; $P < 0.05$; Figure 4a,b) but not in CBMO (35.5 ± 9.5 vs. 13.0 ± 6.0; $n = 6$; $P > 0.05$; Figure 4b) compared with uninfected cells. Interestingly, upregulation was preferentially seen in GFP-positive cells, i.e., those taking part in phagocytosis of *E. coli*-GFP (Figure 4a). The proportion of Bax-positive cells after 4 h of incubation increased in both PBMO (100.0 ± 0.05 vs. 90.0 ± 3.2%) and CBMO (99.9 ± 0.16 vs. 83.2 ± 8.0%; $n = 6$; $P < 0.05$; Figure 4c).

Cytochrome c Was Distributed to Cytosol After Infection With *E. coli*-GFP in PBMO and CBMO

To determine a more specific sign in the intrinsic apoptosis pathway, cytochrome c distribution was analyzed after infection with *E. coli*-GFP by fluorescence microscopy. Infected PBMO and CBMO showed a more cytosolic distribution of cytochrome c compared with uninfected cells (25.0 ± 2.7 vs. 10.7 ± 1.5% and 17.3 ± 1.5 vs. 9.7 ± 1.1%; $n = 3$; Figure 5). However, cytosolic distribution in infected PBMO was more abundant than that in infected CBMO (25.0 ± 2.7 vs. 17.3 ± 1.5%; $n = 3$; $P < 0.05$). After incubation with apoptosis-inducing mitomycin, cytosolic distribution of cytochrome c was even more increased than that in infected PBMO (57.7 ± 5.1% cytosolic distribution after mitomycin).

DISCUSSION

This work aimed at identifying molecular mechanisms involved in diminished apoptosis of CBMO upon infection with *E. coli*-GFP, focusing on the regulation of Bcl-2-proteins. We could show that (i) mRNA expression of the antiapopototic Bcl-xL was significantly upregulated in CBMO and that (ii) mRNA expression of the proapoptotic Bcl-2 protein Bim tended to be higher in PBMO than that in CBMO. (iii) Upon infection, the pro/antiapoptotic balance was skewed toward survival in CBMO and apoptosis in PBMO; (iv) Bax protein expression was enhanced in PBMO as compared with CBMO, while (v) Bcl-xL-expression was slightly diminished in CBMO. (vi) Cytochome c release to the cytosol was enhanced in PBMO compared with CBMO.

Bcl-2-proteins are potent regulators of apoptosis in monocytes (20). Not only the intrinsic but also the extrinsic apoptosis pathway is influenced by these proteins (21).

Upregulation of Bcl-xL mRNA in CBMO upon infection (Figure 2) is in line with previous studies, which showed that infection of macrophages with *E. coli K1* induced *de novo* synthesis of Bcl-xL in macrophages and made them resistant to staurosporin-induced apoptosis (22). Upregulation of Bcl-xL-mRNA in macrophages was also shown upon stimulation with LPS and IFN-γ and blocked NO-induced

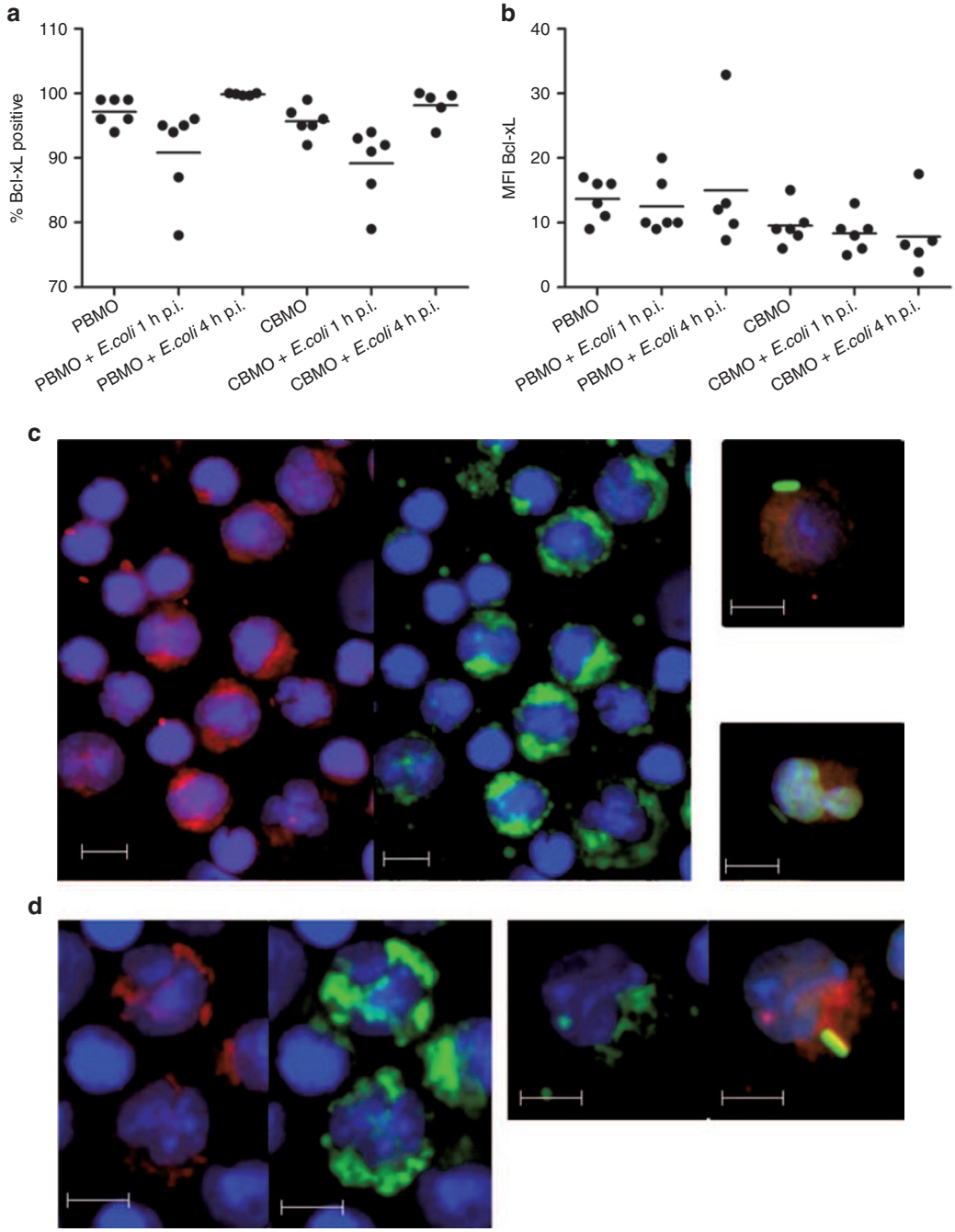

Figure 3. Infection with *E. coli*-GFP had no influence on Bcl-xL protein expression. PBMO and CBMO were infected with *E. coli*-GFP for 1 h. After 1 h and 4 h of further incubation, (**a**) percentage of Bcl-xL–positive cells and (**b**) mean fluorescence intensity (MFI) were analyzed by flow cytometry ($n = 6$, 1 h; $n = 5$, 4 h). Intracellular distribution (mitochondrial or cytosolic) of Bcl-xL was determined by fluorescence microscopy. A representative experiment of (**c**) PBMO and (**d**) CBMO is shown. In **c**, the left panel shows mitochondrial distribution of Bcl-xL in uninfected PBMO, the two pictures on the right side show both mitochondrial distribution of Bcl-xL in infected PBMO. In **d**, the left panel shows uninfected CBMO with mitochondrial distribution of Bcl-xL, and the right panel shows infected CBMO with cytosolic Bcl-xL distribution. Mitochondria: Mito-Tracker Deep Red FM 633 (shown as pseudocolor green) Bcl-xL: anti-Bcl-xL-PE (red). Bar = 10 µm. Bcl, B-cell lymphoma; CBMO, cord blood monocytes; GFP, green fluorescent protein; PBMO, peripheral blood monocytes.

cell death (20). Because of the stronger expression of Bcl-xL as compared with Bcl-2 (23), it is thought to be the prominent antiapoptotic Bcl-2-protein in monocytes. Comparing the expression pattern of Bcl-2 and Bcl-xL in monocytes and lymphocytes, Okada *et al.* (20) found that Bcl-xL was predominantly expressed in differentiating cells. Our data show a higher expression of Bcl-xL in CBMO as compared with PBMO, which might point to a different state of differentiation of these cells, underlining former results concerning their immaturity in phenotype and function (24). Upregulation of Bcl-xL may therefore be an important process in preventing CBMO from PICD as functionally seen.

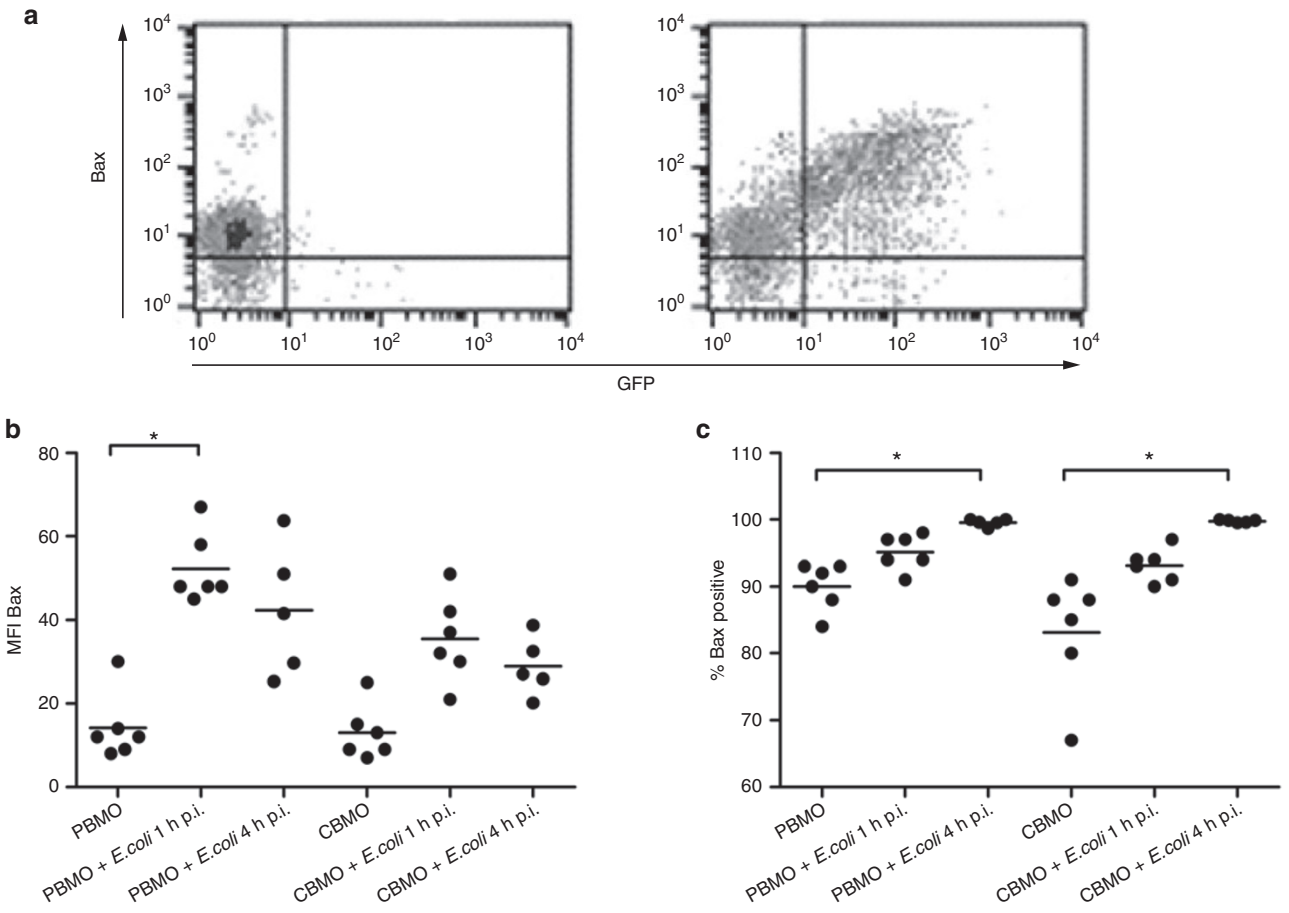

Figure 4. Bax was upregulated in PBMO and CBMO after infection with *E. coli*-GFP. PBMO and CBMO were infected with *E. coli*-GFP for 1 h. After 1 h and 4 h of further incubation, the expression of Bax was analyzed by flow cytometry. Representative density plots of (**a**) uninfected (left) and infected (right) PBMO, (**b**) mean fluorescence intensity (MFI) of GFP-positive events, and (**c**) percentage of all Bax-positive cells are shown ($n = 6$, 1 h; $n = 5$, 4 h; $^*P < 0.05$). CBMO, cord blood monocytes; GFP, green fluorescent protein; PBMO, peripheral blood monocytes.

By contrast, the mRNA of the proapoptotic protein Bim tended to be higher in PBMO than that in CBMO after infection with *E. coli*-GFP (Figure 2c). Upregulation of Bim in macrophages after phagocytosis of bacteria was identified as a mechanism to increase PICD (12,25). Moreover, protein expression of Bax was enhanced in PBMO compared with CBMO after infection. Activated Bax directly leads to permeabilization of the outer mitochondrial membrane and consecutively to a release of cytochrome c into the cytosol (26). The latter can be activated by BH3-only proteins of the Bcl-2 protein family, for example, Bim (27), while Bcl-xL inhibits activation of Bax and therefore mitochondrial membrane permeabilization (15). Thus, all these observations point toward a higher sensitivity of PBMO to apoptosis as compared with CBMO.

However, it was suggested that not the absolute levels of pro- and antiapoptotic proteins determine the cell for apoptosis or survival but rather that the ratio of pro- to antiapoptotic proteins determines cell survival or death (28). Our data indicate that upon infection with *E. coli*-GFP, the pro-/antiapoptotic balance of Bcl-2 family members was skewed toward survival in CBMO and toward apoptosis in PBMO.

Somehow contradictory to this, Bcl-xL protein expression was slightly diminished in CBMO after infection, since mRNA was upregulated in CBMO. The inactive form of Bcl-xL is located in the cytosol or bound to the outer mitochondrial membrane (29,30). Cytosolic Bcl-xL exists as a monomer or homodimer. During apoptosis, Bcl-xL is translocated to the outer mitochondrial membrane, where it forms heterodimers with proapoptotic proteins of the Bcl-family, e.g., Bax (15,19). In this way, Bax can be relocated in the cytosol (31) or Bax-activating factors like Bim, Bid, or PUMA can be inactivated through Bcl-xL (15), which leads to inhibition of apoptosis. The Bcl-xL monoclonal antibody used here can only detect Bcl-xL monomers, because it binds to an epitope in the BH2-domain, which is involved in dimerization (32,33). This may explain the diminished Bcl-xL protein content upon infection in CBMO in our flow cytometric analyses.

In this work, we did not analyze the regulation of the pro-apoptotic Bcl-2 antagonist killer 1 (Bak), which is known to be functionally very similar to Bax, (16) and therefore may also play a role in PICD of monocytes. Total Bak is bound to the outer mitochondrial membrane (16) and is activated upon homodimerization induced by the same stimuli as Bax (34).

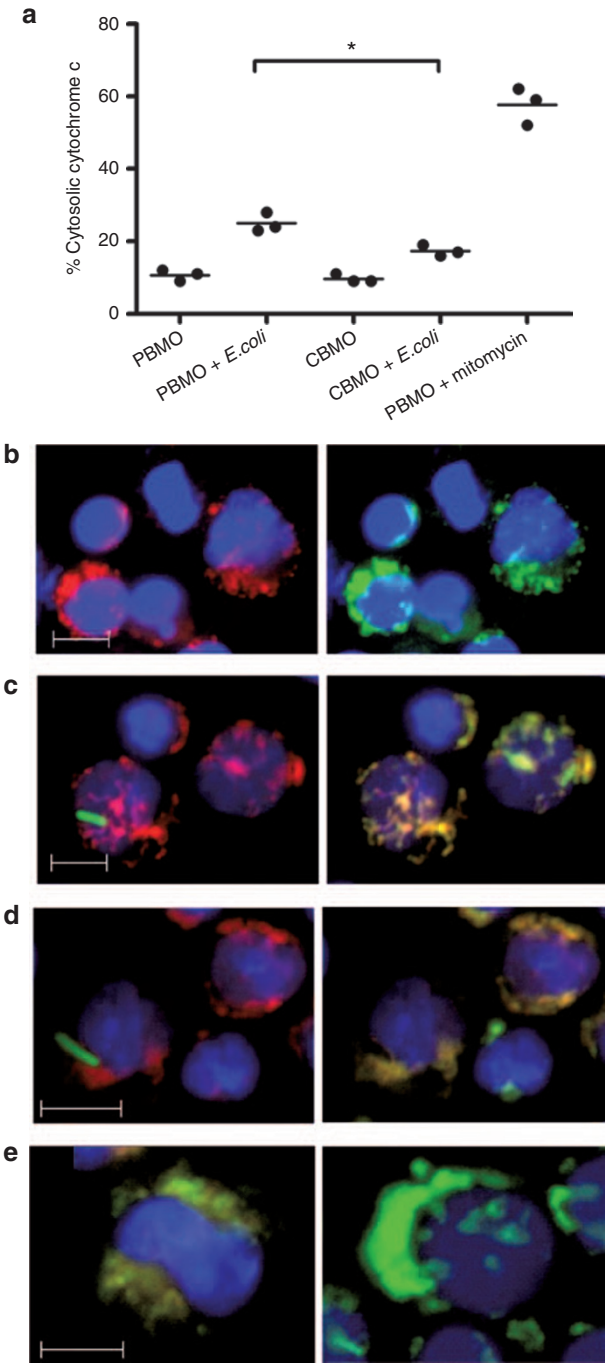

Figure 5. Cytosolic distribution of cytochrome c after infection with *E. coli*-GFP was increased in PBMO compared with CBMO. Cells were infected with *E. coli*-GFP for 1 h. Distribution of cytochrome c was analyzed by fluorescence microscopy. Percentage of cytosolic distributed cytochrome c is shown in **a** ($n = 3$; $^*P < 0.05$). Representative pictures of fluorescence microscopy of (**b**) uninfected PBMO, (**c**) infected PBMO with cytosolic distribution, (**d**) infected PBMO with mitochondrial distribution, and (**e**) mitomycin treated PBMO are given. The two images of **e** show different examples of dying monocytes stained both for cytochrome c. Mitochondria: Mito Tracker Red CMXRos (red, left panel (**b**–**d**)), cytochrome c: anti-cytochrom c-Alexa Fluor 647 (shown as pseudocolor green, right panel (**b**–**d**)), and nuclei: DAPI (blue). Bar = 10 µm. CBMO, cord blood monocytes; GFP, green fluorescent protein; PBMO, peripheral blood monocytes.

Further investigation is needed to determine the role of Bak in PICD.

Indeed, the different regulation of Bcl-2 proteins correlated with the enhanced cytochrome c release into the cytosol in PBMO compared with CBMO (**Figure 5**). Cytochrome c release is thought to be a crucial step toward apoptosis (35) leading to activation of caspase 9 and downstream effector caspases (14). Cytochrome c is located in the mitochondrial intermembrane space (34) and may be released upon mitochondrial outer membrane permeabilization by activated Bax or Bak (14). We could demonstrate cytosolic distribution of cytochrome c in both CBMO and PBMO (**Figure 5**). However, Jourdain *et al.* (34) suggested that only total release of cytochrome c leads to apoptosis, while a partial release might not be sufficient for caspase activation. We therefore speculate that cytochrome c release might be hampered in CBMO, possibly because of antiapoptotic distribution of Bcl-2 proteins, while in PBMO, the amount of released cytochrome c may be sufficient for apoptosis induction. This is in line with the previous results showing diminished caspase 9 activation in CBMO upon *E. coli* infection and strong activation of caspase 9 in activated PBMO (8).

The results presented here may give further insights into the mechanisms preventing CBMO from PICD and may extend the understanding of the different susceptibility of PBMO and CBMO toward apoptosis. Yet, only alterations in the activation of the extrinsic apoptosis pathway of CBMO have been described, i.e., a diminished release and impact of the two death ligands CD95L (13) and TNF-α (36). We now show that the regulation of Bcl-2 family proteins and the following steps in the intrinsic apoptosis signaling pathway also differ between CBMO and PBMO.

Reduced apoptosis of activated immune effector cells, such as monocytes, has been described as pathophysiologically relevant not only in autoimmune diseases like systemic juvenile idiopathic arthritis(37) but also in septic patients, leading to excessive and prolonged inflammation and organ damage (11). Sustained inflammation was identified as crucial in the etiology of bronchopulmonary dysplasia and periventricular leukomalacia, which exclusively manifest during the neonatal

Table 2. Primer for qRT-PCR of Bcl-proteins

Gene	Sense	Antisense
Bcl-xL	gta gtg aat gaa ctc ttc cg	gta tcc cag ccg ccg ttc tc
Bim	gag cca caa gac agg agc	cca ttg cac tga gat agt gg
Bid	tgg tgt ttg gct tcc tcc aa	gaa tct gcc tct att ctt ccc
Mcl-1	ctc tca ttt ctt ttg gtg cct	att cct gat gcc acc ttc ta
Bax	gac gtg ggc att ttt ctt ac	gtg tcc cga agg agg ttt at
PDH	ggt ttc cca ttc aag acc tg	tgg ttt cca tgt cca ttg gt
SDHA	aga agc cct ttg agg agc a	cga tta cgg gtc tat att cca ga
PPIB	aag ggg ccc aaa gtc acc gtc aag	ggg gaa gcg ctc acc gta gat gc

Bcl, B-cell lymphoma; PDH, pyruvatdehydrogenase; PPIB, peptidyl-prolyl-isomerase B; SDHA, succinate dehydrogenase.

period. Thus, controlling inflammation seems to be particularly important in the neonate, since developing organs like lungs and brain may be susceptible to inflammatory injury (2,4,5). Although our experiments were performed with *ex vivo* materials from patients, clinical studies are needed to get a profound knowledge of the *in vivo* regulation of Bcl-2 proteins in neonatal infection. A detailed knowledge of apoptosis signaling following phagocytosis in neonatal monocytes may be essential for developing new antiinflammatory strategies.

METHODS

Patients

The study protocol was approved by the Ethics Committees of Tuebingen University Hospital. All mothers gave written informed consent prior to going into labor. All term neonates were delivered spontaneously and did not exhibit signs of infection, as defined by clinical status, white blood cell count, and C-reactive protein. Mothers with amnion infection and prolonged labor were excluded. Umbilical cord blood was placed in heparin-coated tubes (4 international units/ml blood; heparin from Meduna, Isernhagen, Germany), immediately following cord ligation. Randomly selected, unrelated adults donated blood and served as controls.

Reagents

Monoclonal antibodies (mAb) to CD14 (MFP9) were from BD Biosciences (Heidelberg, Germany), antiBcl-xL (H-5) were from Santa Cruz Biotechnology (Heidelberg, Germany), Ig-matched controls (IgG1, IgG2b) and Fix-and-Perm-Solution were from BD Biosciences. AntiBax (B-9) mAB was purchased from Santa Cruz Biotechnology. Propidium iodide (13), isopropyl-β-D-thiogalactopyranosid, and antibiotics were purchased from Sigma (Munich, Germany).

Cell Cultures

Peripheral blood mononuclear cells (PBMC) and cord-blood mononuclear cells (CBMC) were isolated by density gradient centrifugation (Biochrom AG, Berlin, Germany) as described (38). Washed cells were resuspended in VLE RPMI-1640 (Biochrom), containing 10% heat-inactivated fetal calf serum (Biochrom) at 2×10^6 cells/ml in flat bottom 24-well cell culture plates (Costar, Bodenheim, Germany).

Purification of Monocytes

Monocytes were separated by positive selection using magnetic cell sorting (MACS) CD14 beads (Miltenyi Biotec, Bergisch Gladbach, Germany) according to the manufacturer's instructions. The purity of the resulting population was >92% CD14-positive cells as detected by flow cytometry.

Bacterial Culture

E. coli DH5α, an encapsulated K12 laboratory strain, carrying the green fluorescent protein (*gfp*)-mut2 gene (39), was a kind gift of Prof Christoph Dehio, University of Basel, Switzerland, and used for all infection assays (*E. coli*-GFP). Bacteria were freshly grown in Lennox-L-Broth-medium (Invitrogen, Karlsruhe, Germany) until early logarithmic growth, resuspended in phosphate-buffered saline (PBS, Biochrom) and used immediately.

Phagocytosis Assay

The phagocytosis assay was carried out as previously described (38). Incubation was performed for 60 min at a multiplicity of infection of 50:1. For analysis of postphagocytic reactions, washed cells were cultured in RPMI supplemented with 10% fetal calf serum and gentamycin (Sigma; 200 μg/ml).

DNA Fragmentation

DNA fragmentation was assessed according to Nicoletti (8,40). Washed cells were slowly resuspended in 2 ml of −20 °C ethanol 70% under continuous vortexing and stored for 4 h at −20 °C. Cells were washed twice, resuspended in 50 μl PBS containing 13 kunitz units RNase (DNase free; Sigma), and incubated for 15 min at 37 °C. Thereafter 180 μl of propidium iodide (70 μg/ml) were added, incubated for 20 min, and immediately analyzed.

Intracellular Staining of Bcl-2 Family Members

After removal of bacteria, cells were washed with buffer (PBS with 0.1% bovine serum albumin (Sigma) and 0.1% sodium azide (Sigma)). Hundred microliters of Fix-and-Perm-Solution (BD Biosciences) was added for 20 min. Cells were washed with PBS with 0.5% bovine serum albumin, 0.1% Saponin (Sigma), 0.02% sodium azide, stained with anti-Bax, anti-Bcl-xL, or isotype control for 30 minutes, washed twice, and analyzed.

Fluorescence Microscopy

Monocytes were stained with DAPI (1 μg/ml; Merck, Darmstadt, Germany). The following antibody combinations were used: anti-Bcl-xL-PE and Mito-Tracker Deep Red FM 633 or Mito Tracker Red CMXRos (Invitrogen) and anti-cytochrome c and Alexa Fluor 647 (both from BD Biosciences). Emission of PE-fluorocomes and Mito Tracker Red CMXRos were detected through appropriate single pass filters. Cells were centrifuged onto class slides with a Cytospin-16A-centrifuge (Hettich, Tuttlingen, Germany; 300×*g*, 5 min), mounted in Fluoprep-mounting-medium (bioMérieux, Marcy l´Etoile, France) and analyzed with an Axioplan-2 microscope (Carl Zeiss, Jena, Germany) with the help of Isis-imaging software (MetaSytems, Altlussheim, Germany). For better visualization, pseudocolors were used (see figure legends).

mRNA Quantification of Bcl-2 Family Members

Total mRNA was extracted of monocytes with the RNeasy Mini Kit (Quiagen, Hilden, Germany) according to the manufacturer's instructions and treated with DNAse (Fermentas, St Leon-Roth, Germany). First-strand cDNA was synthesized using Reverse Transcriptase SuperScript (Invitrogen, Karlsruhe, Germany). cDNA was preamplified with TaqMan PreAmp Mastermix (Invitrogen) according to the manufacturer's instructions. qRT-PCR was performed using a LightCycler 3.0 (Roche Applied Sciences, Mannheim, Germany) and Light Cycler DNA Master Sybr Green I (Roche Applied Sciences, Mannheim, Germany) for the amplification of genes of the Bcl-protein-family. For primers, see **Table 2**.

Fluorescence signals were expressed in crossing point values. The specificity of amplification was validated by a single peak in the melting curves. Peptidyl-prolyl-isomerase B, succinate dehydrogenase, and pyruvatdehydrogenase served as housekeeping genes. All experiments were performed in triplicate. Relative expressions were calculated using REST2009 software (Technical University Munich, Munich, Germany).

Statistical Analysis

Analyses were done with GraphPad Prism 5.04 (GraphPad Software, La Jolla, CA) using one-way ANOVA followed by *post hoc* tests. A P value of <0.05 was considered statistically significant. While doing the experiments for the protein expression of Bcl-xL and Bax, the laser of the flow cytometer was renewed. Obtained MFI values were adjusted.

SUPPLEMENTARY MATERIAL

Supplementary material is linked to the online version of the paper at http://www.nature.com/pr

ACKNOWLEDGMENTS

The authors thank Silke Schulz (Department of Gynaecology, University of Duesseldorf, Germany) and Michael Walter (Institute of Genetics, Tuebingen University) for their help with PCR protocols.

STATEMENT OF FINANCIAL SUPPORT

This work was supported by the Research Fund of the Medical Faculty of Tuebingen University, Tuebingen, Germany, grant no. F.1275143.

Disclosure: The authors have no conflicts of interest.

REFERENCES

1. Stoll BJ, Hansen NI, Bell EF, et al.; Eunice Kennedy Shriver National Institute of Child Health and Human Development Neonatal Research Network. Neonatal outcomes of extremely preterm infants from the NICHD Neonatal Research Network. Pediatrics 2010;126:443–56.
2. Thomas W, Speer CP. Chorioamnionitis: important risk factor or innocent bystander for neonatal outcome? Neonatology 2011;99:177–87.
3. Leviton A, Fichorova R, Yamamoto Y, et al. Inflammation-related proteins in the blood of extremely low gestational age newborns. The contribution of inflammation to the appearance of developmental regulation. Cytokine 2011;53:66–73.
4. Hentschel J, Berger TM, Tschopp A, Müller M, Adams M, Bucher HU; Swiss Neonatal Network. Population-based study of bronchopulmonary dysplasia in very low birth weight infants in Switzerland. Eur J Pediatr 2005;164:292–7.
5. Schlapbach LJ, Aebischer M, Adams M, et al.; Swiss Neonatal Network and Follow-Up Group. Impact of sepsis on neurodevelopmental outcome in a Swiss National Cohort of extremely premature infants. Pediatrics 2011;128:e348–57.
6. Medzhitov R, Janeway C Jr. Innate immunity. N Engl J Med 2000;343:338–44.
7. Feig C, Peter ME. How apoptosis got the immune system in shape. Eur J Immunol 2007;37:Suppl 1:S61–70.
8. Gille C, Leiber A, Spring B, et al. Diminished phagocytosis-induced cell death (PICD) in neonatal monocytes upon infection with Escherichia coli. Pediatr Res 2008;63:33–8.
9. DeLeo FR. Modulation of phagocyte apoptosis by bacterial pathogens. Apoptosis 2004;9:399–413.
10. Hotchkiss RS, Nicholson DW. Apoptosis and caspases regulate death and inflammation in sepsis. Nat Rev Immunol 2006;6:813–22.
11. Giamarellos-Bourboulis EJ, Routsi C, Plachouras D, et al. Early apoptosis of blood monocytes in the septic host: is it a mechanism of protection in the event of septic shock? Crit Care 2006;10:R76.
12. Kirschnek S, Ying S, Fischer SF, et al. Phagocytosis-induced apoptosis in macrophages is mediated by up-regulation and activation of the Bcl-2 homology domain 3-only protein Bim. J Immunol 2005;174:671–9.
13. Gille C, Dreschers S, Leiber A, et al. The CD95/CD95L pathway is involved in phagocytosis-induced cell death of monocytes and may account for sustained inflammation in neonates. Pediatr Res 2013;73(4 Pt 1):402–8.
14. Autret A, Martin SJ. Emerging role for members of the Bcl-2 family in mitochondrial morphogenesis. Mol Cell 2009;36:355–63.
15. Billen LP, Kokoski CL, Lovell JF, Leber B, Andrews DW. Bcl-XL inhibits membrane permeabilization by competing with Bax. PLoS Biol 2008;6:e147.
16. Chipuk JE, Moldoveanu T, Llambi F, Parsons MJ, Green DR. The BCL-2 family reunion. Mol Cell 2010;37:299–310.
17. Ghiotto F, Fais F, Bruno S. BH3-only proteins: the death-puppeteer's wires. Cytometry A 2010;77:11–21.
18. Gille Ch, Leiber A, Mundle I, et al. Phagocytosis and postphagocytic reaction of cord blood and adult blood monocyte after infection with green fluorescent protein-labeled Escherichia coli and group B Streptococci. Cytometry B Clin Cytom 2009;76:271–84.
19. Jeong SY, Gaume B, Lee YJ, et al. Bcl-x(L) sequesters its C-terminal membrane anchor in soluble, cytosolic homodimers. EMBO J 2004;23:2146–55.
20. Okada S, Zhang H, Hatano M, Tokuhisa T. A physiologic role of Bcl-xL induced in activated macrophages. J Immunol 1998;160:2590–6.
21. Croker BA, O'Donnell JA, Nowell CJ, et al. Fas-mediated neutrophil apoptosis is accelerated by Bid, Bak, and Bax and inhibited by Bcl-2 and Mcl-1. Proc Natl Acad Sci USA 2011;108:13135–40.
22. Sukumaran SK, Selvaraj SK, Prasadarao NV. Inhibition of apoptosis by Escherichia coli K1 is accompanied by increased expression of BclXL and blockade of mitochondrial cytochrome c release in macrophages. Infect Immun 2004;72:6012–22.
23. Ohta K, Iwai K, Kasahara Y, et al. Immunoblot analysis of cellular expression of Bcl-2 family proteins, Bcl-2, Bax, Bcl-X and Mcl-1, in human peripheral blood and lymphoid tissues. Int Immunol 1995;7:1817–25.
24. Orlikowsky TW, Spring B, Dannecker GE, Niethammer D, Poets CF, Hoffmann MK. Expression and regulation of B7 family molecules on macrophages (MPhi) in preterm and term neonatal cord blood and peripheral blood of adults. Cytometry B Clin Cytom 2003;53:40–7.
25. Steimer DA, Boyd K, Takeuchi O, Fisher JK, Zambetti GP, Opferman JT. Selective roles for antiapoptotic MCL-1 during granulocyte development and macrophage effector function. Blood 2009;113:2805–15.
26. Dejean LM, Martinez-Caballero S, Guo L, et al. Oligomeric Bax is a component of the putative cytochrome c release channel MAC, mitochondrial apoptosis-induced channel. Mol Biol Cell 2005;16:2424–32.
27. Gallenne T, Gautier F, Oliver L, et al. Bax activation by the BH3-only protein Puma promotes cell dependence on antiapoptotic Bcl-2 family members. J Cell Biol 2009;185:279–90.
28. Oltvai ZN, Milliman CL, Korsmeyer SJ. Bcl-2 heterodimerizes *in vivo* with a conserved homolog, Bax, that accelerates programmed cell death. Cell 1993;74:609–19.
29. Hsu YT, Wolter KG, Youle RJ. Cytosol-to-membrane redistribution of Bax and Bcl-X(L) during apoptosis. Proc Natl Acad Sci USA 1997;94:3668–72.
30. Petros AM, Olejniczak ET, Fesik SW. Structural biology of the Bcl-2 family of proteins. Biochim Biophys Acta 2004;1644:83–94.
31. Edlich F, Banerjee S, Suzuki M, et al. Bcl-x(L) retrotranslocates Bax from the mitochondria into the cytosol. Cell 2011;145:104–16.
32. Sedlak TW, Oltvai ZN, Yang E, et al. Multiple Bcl-2 family members demonstrate selective dimerizations with Bax. Proc Natl Acad Sci USA 1995;92:7834–8.
33. Yin XM, Oltvai ZN, Korsmeyer SJ. BH1 and BH2 domains of Bcl-2 are required for inhibition of apoptosis and heterodimerization with Bax. Nature 1994;369:321–3.
34. Jourdain A, Martinou JC. Mitochondrial outer-membrane permeabilization and remodelling in apoptosis. Int J Biochem Cell Biol 2009;41:1884–9.
35. Liu X, Kim CN, Yang J, Jemmerson R, Wang X. Induction of apoptotic program in cell-free extracts: requirement for dATP and cytochrome c. Cell 1996;86:147–57.
36. Dreschers S, Gille C, Haas M, et al. Infection-induced bystander-apoptosis of monocytes is TNF-alpha-mediated. PLoS One 2013;8:e53589.
37. Srivastava S, Macaubas C, Deshpande C, et al. Monocytes are resistant to apoptosis in systemic juvenile idiopathic arthritis. Clin Immunol 2010;136:257–68.
38. Gille C, Spring B, Tewes L, Poets CF, Orlikowsky T. A new method to quantify phagocytosis and intracellular degradation using green fluorescent protein-labeled Escherichia coli: comparison of cord blood macrophages and peripheral blood macrophages of healthy adults. Cytometry A 2006;69:152–4.
39. Dehio M, Knorre A, Lanz C, Dehio C. Construction of versatile high-level expression vectors for Bartonella henselae and the use of green fluorescent protein as a new expression marker. Gene 1998;215:223–9.
40. Nicoletti I, Migliorati G, Pagliacci MC, Grignani F, Riccardi C. A rapid and simple method for measuring thymocyte apoptosis by propidium iodide staining and flow cytometry. J Immunol Methods 1991;139:271–9.